

University of Groningen

Diffusion weighted imaging in the liver

Kele, Petra G.; van der Jagt, Eric J.

Published in:
World Journal of Gastroenterology

DOI:
[10.3748/wjg.v16.i13.1567](https://doi.org/10.3748/wjg.v16.i13.1567)

IMPORTANT NOTE: You are advised to consult the publisher's version (publisher's PDF) if you wish to cite from it. Please check the document version below.

Document Version
Publisher's PDF, also known as Version of record

Publication date:
2010

[Link to publication in University of Groningen/UMCG research database](#)

Citation for published version (APA):
Kele, P. G., & van der Jagt, E. J. (2010). Diffusion weighted imaging in the liver. *World Journal of Gastroenterology*, 16(13), 1567-1576. <https://doi.org/10.3748/wjg.v16.i13.1567>

Copyright

Other than for strictly personal use, it is not permitted to download or to forward/distribute the text or part of it without the consent of the author(s) and/or copyright holder(s), unless the work is under an open content license (like Creative Commons).

Take-down policy

If you believe that this document breaches copyright please contact us providing details, and we will remove access to the work immediately and investigate your claim.

Downloaded from the University of Groningen/UMCG research database (Pure): <http://www.rug.nl/research/portal>. For technical reasons the number of authors shown on this cover page is limited to 10 maximum.



Paul E Sijens, PhD, Associate Professor, Series Editor

Diffusion weighted imaging in the liver

Petra G Kele, Eric J van der Jagt

Petra G Kele, Eric J van der Jagt, Department of Radiology, University Medical Center Groningen, University of Groningen, 9700 RB Groningen, The Netherlands

Author contributions: Kele PG wrote the manuscript; van der Jagt EJ, expert in abdominal radiology, commented the manuscript.

Correspondence to: Petra G Kele, MD, Research Officer, Department of Radiology, University Medical Center Groningen, University of Groningen, 9700 RB Groningen, The Netherlands. p.g.kele@rad.umcg.nl

Telephone: +31-50-3611098 Fax: +31-50-3617008

Received: February 3, 2010 Revised: February 25, 2010

Accepted: March 4, 2010

Published online: April 7, 2010

This review focuses on the most common applications of DWI in the liver.

© 2010 Baishideng. All rights reserved.

Key words: Diffusion; Magnetic resonance imaging; Diffusion weighted imaging; Benign neoplasms; Liver neoplasms

Peer reviewer: Paul E Sijens, PhD, Associate Professor, Radiology, UMCG, Hanzeplein 1, 9713GZ Groningen, The Netherlands

Kele PG, van der Jagt EJ. Diffusion weighted imaging in the liver. *World J Gastroenterol* 2010; 16(13): 1567-1576 Available from: URL: <http://www.wjgnet.com/1007-9327/full/v16/i13/1567.htm> DOI: <http://dx.doi.org/10.3748/wjg.v16.i13.1567>

Abstract

Diffusion weighted magnetic resonance imaging (DWI) is an imaging technique which provides tissue contrast by the measurement of diffusion properties of water molecules within tissues. Diffusion is expressed in an apparent diffusion coefficient (ADC), which reflects the diffusion properties unique to each type of tissue. DWI has been originally used in neuroradiology. More recently, DWI has increasingly been used in addition to conventional unenhanced and enhanced magnetic resonance imaging (MRI) in other parts of the body. The reason for this delay was a number of technical problems inherent to the technique, making DWI very sensitive to artifacts, which had to be overcome. With assessment of ADC values, DWI proved to be helpful in characterization of focal liver lesions. However, DWI should always be used in conjunction to conventional MRI since there is considerable overlap between ADC values of benign and malignant lesions. DWI is useful in the detection of hepatocellular carcinoma in the cirrhotic liver and detection of liver metastases in oncological patients. In addition, DWI is a promising tool in the prediction of tumor responsiveness to chemotherapy and the follow-up of oncological patients after treatment, as DWI may be capable of detecting recurrent disease earlier than conventional imaging.

INTRODUCTION

Magnetic resonance imaging (MRI) is an imaging technique which is used to visualize the internal structure and function of the body. MRI provides excellent tissue contrast, which is much greater than that of any other imaging modality^[1,2]. Tissue contrast is realized by a wide range of pulse sequences. For example, tissue contrast on T1- and T2-weighted images is based on the rate at which signals from protons in water molecules in a static magnetic field decay following excitation by a sequence of radiofrequency (RF) pulses. Diffusion weighted imaging (DWI) is another mechanism for developing image contrast and relies on changes in the diffusion properties of water molecules in tissues. DWI is a widely accepted technique in neuroradiology for detecting early ischemia in cerebrovascular accidents and characterization of brain tumors and intracranial infections^[1-3]. The use of DWI in other parts of the body is relatively new, but very promising for the detection and differentiation of benign and malignant lesions, imaging for dissemination (i.e. staging) in oncological patients before treatment and

for follow-up after treatment of liver tumors. Besides this, DWI is thought to be capable of predicting the response to therapy of malignant tumors (especially chemotherapy)^[4].

BASIC PRINCIPLES OF DWI

Diffusion

Diffusion is a physical property, which describes the microscopic random movement of (water) molecules driven by their internal thermal energy. This movement is known as Brownian motion. In biological tissues, water diffusion is movement of water molecules in intracellular, extracellular and intravascular spaces. Diffusion is affected by the biophysical properties of tissue cell organization (cell membranes, fibers and macromolecules), density, microstructure and microcirculation. Intracellular water diffusion is more hindered than that in the extracellular spaces which are lacking natural barriers. Pathological processes which change the volume ratio or physical nature of intra- and extracellular spaces affect the diffusion of water molecules. Restricted or impeded diffusion is seen in tissues with high cellularity, e.g. tumors, abscesses, fibrosis and cytotoxic edema. Relative free or unimpeded diffusion is encountered in tissues with low cellularity or tissues with disrupted cell membranes, for example in cysts and necrotic tissues^[3-5] (Figure 1A and B).

DWI

DWI relies on measuring diffusion of water molecules in the tissue by MRI. It uses a pulse sequence (T2-weighted spin echo sequence) and 2 strong motion probing gradients on either side of the 180° refocusing pulse, known as the Stejskal-Tanner sequence. The first gradient, prior to the 180° RF pulse is the dephasing (diffusion sensitizing) gradient. The second gradient, after the RF pulse, is the rephasing gradient. In tissues with restricted diffusion, the effect of the dephasing gradient is cancelled out by the rephasing gradient. This causes little impact on the overall T2 decay, reflected as a maintained T2 signal in the tissue. When diffusion is not impeded, water molecules can move a considerable distance between the dephasing and rephasing gradients. The mobile water molecules will not be fully rephased and a reduction in overall T2 signal intensity follows.

DWI is sensitive to very small scale motion of water molecules at a microscopic level. The sensitivity of a DWI sequence is characterized by its b-value, expressed in s/mm². The b-value summarizes the influence of the gradients in DWI. The higher the b-value, the more sensitive the sequence is to diffusion effects. DWI is performed with at least two b-values. Diffusion is quantitatively reflected in a diffusion coefficient. The diffusion coefficient is related to the molecular mobility of water molecules and reflects tissue properties such as the size of the extracellular space, viscosity and cellularity. Diffusion coefficients in DWI are reflected in the *apparent diffusion coefficient* (ADC, expressed in mm²/s), apparent because it is a mean value of diffusion contributed by

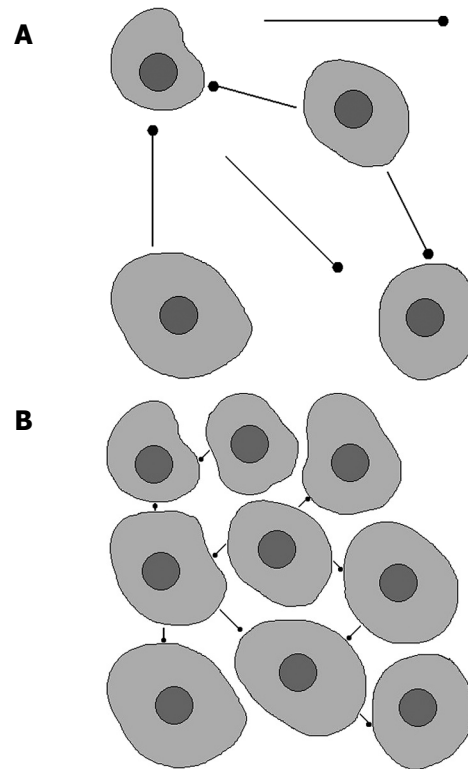


Figure 1 Brownian movements in hypocellular (A) and hypercellular (B) environment. A: Tissue with low cellularity permits movement of the water molecules; B: Tissue with high cellularity restricts the movement of water molecules.

movement of intracellular, extracellular and vascular water molecules within an image voxel (volumetric pixel) at different b-values. Analysis of ADC is an automated process, available as an application on most scanners or workstations. Calculation of ADC is made for each voxel of an image and can be displayed as a parametric (ADC) map. ADC measurements are then recorded for a given region by drawing regions of interest (ROIs) on the ADC map. Low ADC values mean restricted diffusion, thus in tissues which are highly cellular. High ADC values are seen in areas with relative free diffusion, thus in tissues with low cellularity^[1,3-5].

Problems encountered in DWI

DWI can be performed with different techniques, including spin-echo (SE), fast spin echo (FSE), gradient echo (GE) and echo-planar imaging (EPI). EPI is the gold standard DWI technique. When DWI is performed in the body, scanning can be carried out with free breathing, breath hold or respiratory triggered. There are some important limitations of DWI^[2,6].

Firstly, the signal-to-noise ratio (SNR, describes the relative contributions of the true signal and background noise to a detected signal) and spatial resolution are low due to hardware limitations and high bandwidth (a measure of frequency range, the range between the highest and lowest frequency allowed in the signal), inherent to the technique and EPI sequence. SNR will be decreased in incomplete spin echo formation, as is the case with

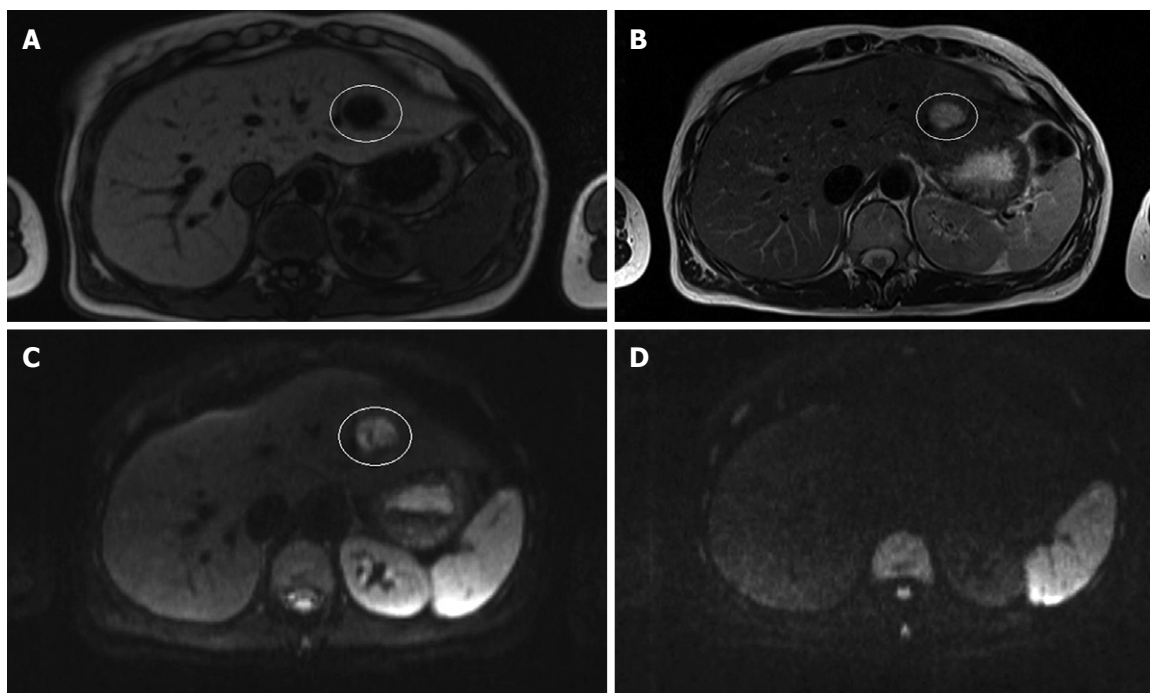


Figure 2 Magnetic resonance imaging (MRI) and diffusion weighted imaging (DWI) of a cyst. A: T1-weighted MRI; B: T2-weighted MRI; C: Diffusion weighted image (b-value 50 s/mm²); D: Diffusion weighted image (b-value 1000 s/mm²) in a 33-year old woman with multiple liver lesions. The cyst is hypo-intense on the T1-weighted image, hyper-intense on the T2-weighted image and the diffusion weighted image at a b-value 50 s/mm². Note that the cyst totally disappears on the diffusion weighted image at a b-value 1000 s/mm².

the most common DWI technique, the EPI sequence. SNR can be increased, but then spatial resolution is sacrificed^[2,3,6-8].

Secondly, DWI is susceptible to a number of artifacts. Ghosting images and blurring may arise from motion, caused by respiratory, cardiac and voluntary movements. Tissue contrast is maintained during free-breathing scanning, but breath hold and respiratory triggered techniques reduce image blurring. Breath hold scans have very short acquisition times of 20-30 s (i.e. the time the patient holds his or her breath) and are theoretically less likely to be degraded by motion-related artifacts. A disadvantage of breath-hold scanning is that the patient needs to hold his or her breath for a considerable time, which may be difficult when the physical condition does not allow him or her to do so. Respiratory triggering will make the acquisition time of the images longer (5 min), especially when the patient is breathing irregularly or slowly, but this is a minimal time penalty. Respiratory triggering provides substantially improved signal, spatial resolution and the ADC values are comparable to breath-hold DWI. In respiratory triggering, multiple b-values can be used to reduce errors in ADC calculation^[2,3,6,7,9-11].

Motion artifacts caused by the heart beating alter ADC in the left lobe of the liver, making measurements unreliable. Cardiac motion can be overcome by using electrocardiographic-triggering, but cardiac gating is not always reliable and increases acquisition times significantly^[2,3,6,7,12].

Susceptibility artifacts are due to magnetic field inhomogeneity (to be overcome by shimming techniques) or metal artifacts and are seen as bright spots, spatial

distortion or signal drop out. Susceptibility artifacts occur especially in fast imaging techniques like EPI^[2,6,7].

Artifacts caused by air-tissue interfaces or fat-water interfaces (chemical shift) appear as black or bright bands at the edge of an anatomical structure. Other artifacts are eddy currents, resulting from the rapid on and off switching of the gradients, leading to geometrical distortion and image shearing artifacts^[2,6,7].

Pathological diffusion

When evaluating diffusion on DWI images, the radiologist focuses on the measurement of extracellular diffusion. As mentioned earlier, the higher the cellularity in a tissue, the less far is extracellular water able to diffuse during the MR observation period without being blocked by cell membranes. Highly cellular tissues provide a short path of diffusion, resulting in low ADC values, as is seen in solid liver lesions and abscesses. Low cellularity means that there are fewer structural barriers, making the diffusion path longer. This results in high ADC values as is seen in cysts and necrotic lesions. In summary, ADC maps, derived from DWI provide a non-invasive measure of cellularity. This makes DWI a potential tool in diagnosis, treatment planning and monitoring, especially in oncology^[3-5]. Examples of different types of lesions and their diffusion weighted images are seen in Figures 2-5.

DWI IN THE LIVER

There are an increasing number of studies dealing with quantitative measurements of ADC in liver lesions, but

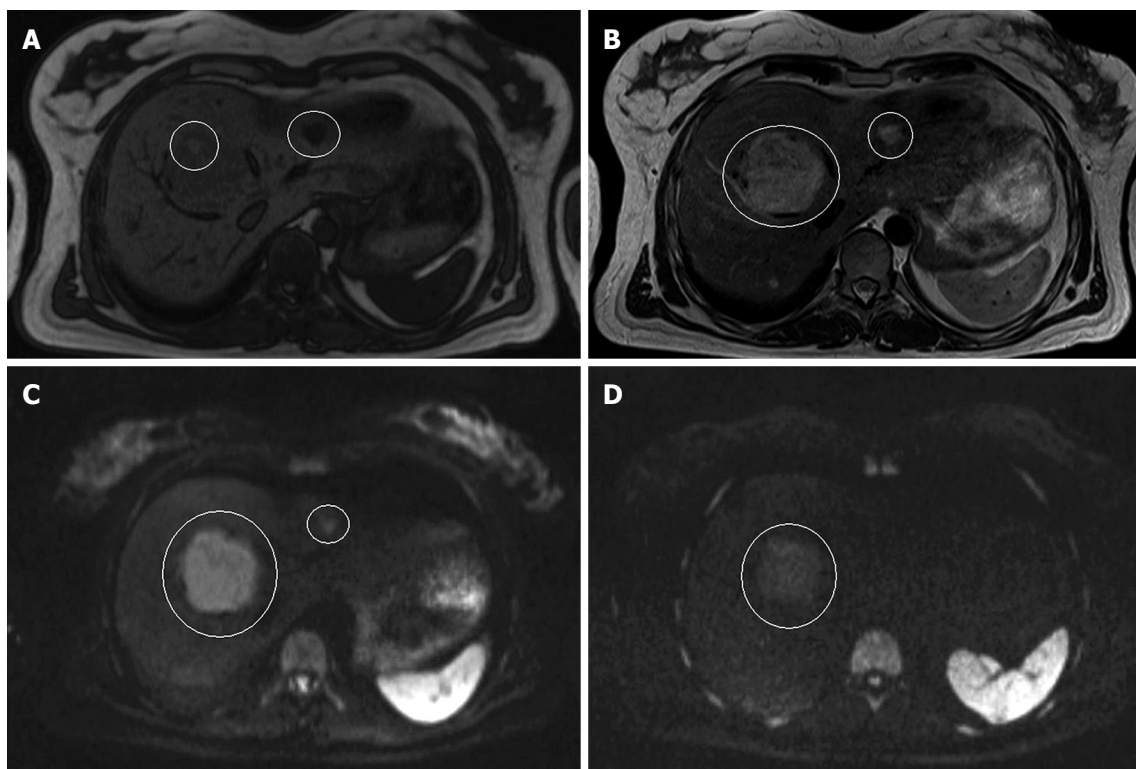


Figure 3 MRI and DWI of an adenoma and a hemangioma. A: T1-weighted MRI; B: T2-weighted MRI; C: Diffusion weighted image (b-value 50 s/mm²); D: Diffusion weighted image (b-value 1000 s/mm²) in a 41-year-old women with multiple liver lesions. The large lesion in segment 8 is an adenoma and the small one in segment 2-3 is a hemangioma. On the T1-weighted image, the adenoma is slightly hypo-intense to the normal liver parenchyma, and hyper-intense on the T2-weighted image. On the diffusion weighted images, it remains hyper-intense at both b-values. The hemangioma is also hypo-intense on the T1-weighted image and hyper-intense on the T2-weighted image. However, in contrast to the adenoma, it totally disappears at a b-value of 1000 mm/s².

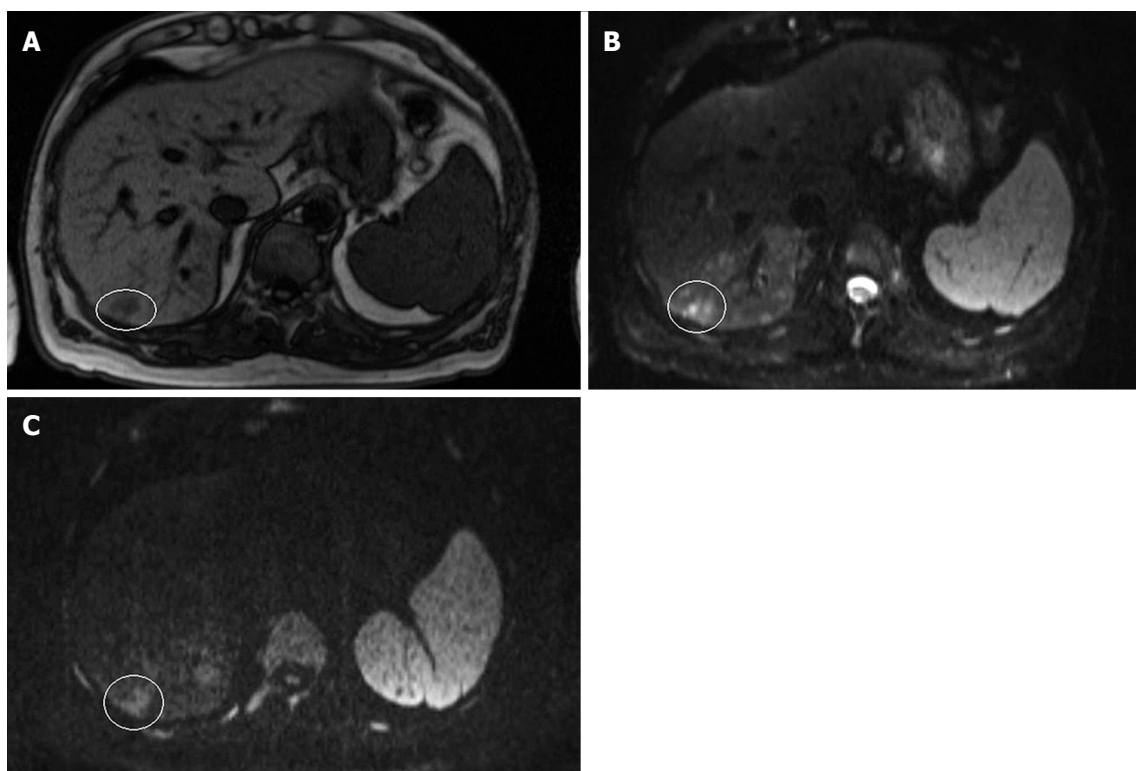


Figure 4 MRI and DWI of hepatocellular carcinoma. A: T1-weighted; B: DWI (b-value 50 s/mm²); C: Diffusion weighted image (b-value 1000 s/mm²) in a 67-year-old male with hemophilia, hepatitis C-based liver cirrhosis and HCC in segment 7. The HCC is hypo-intense on the T1-weighted image and hyper-intense on the diffusion weighted images at both b-values. Note that the lesion remains hyper-intense on the image with a b-value 1000 s/mm².

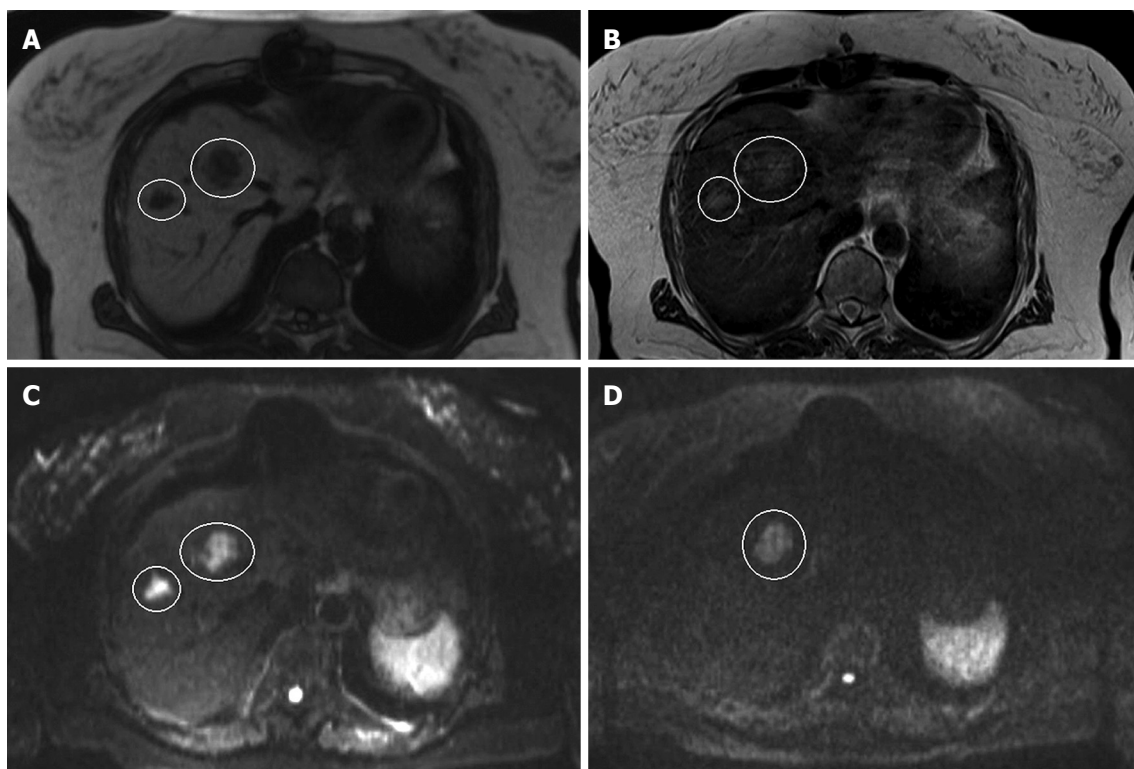


Figure 5 MRI and DWI of hepatic metastases. A: T1-weighted; B: T2-weighted; C: Diffusion weighted image (b-value 50 s/mm²); D: Diffusion weighted image (b-value 1000 s/mm²) in a 74-year-old woman with a history of rectal cancer, recently diagnosed with lung and liver metastases in segment 4 and 8, respectively. The lesions are hypo-intense to the liver parenchyma on the T1-weighted image and hyper-intense on the T2-weighted image. On the diffusion weighted image at a b-value 50 s/mm², both lesions appear hyper-intense, but at a b-value 1000 s/mm², only the lesion in segment 4 remains hyper-intense. The lesion in segment 8 has completely disappeared.

there are as many discrepancies in the reported ADC values (Table 1). This is often associated with the choice of b-values and other technical parameters. Low b-values lead to overestimation of the ADC due to the contribution of perfusion to the diffusion measurement. Large b-values underestimate ADC due to increasing contributions from low ADC components and SNR.

DWI as a tool for characterization of liver lesions

Several studies have suggested that the measurement of ADC values is useful in the characterization of focal liver lesions^[13-26]. Reduced ADC values have been reported for most malignant tumors. This finding is thought to be the result of cellular membranes impeding the mobility of water molecules. However, solid benign lesions, which are also highly cellular, exhibit decreased ADC values as well. Abscesses do so too because their viscous content with bacteria, inflammatory cells, mucoid proteins and cell debris result in restricted diffusion, thus low ADC values. On the other hand, necrotic and cystic malignancies show high ADC values resulting from larger diffusion distances as a consequence of lost membrane integrity. Benign lesions as simple cysts and hemangiomas show high ADC values because of their liquid content and large extracellular spaces. However, ADC values cannot discriminate between solid benign and malignant lesions, since there is considerable overlap. According to Feuerlein *et al*^[15], the pretest probability of malignancy is very important in the determination to which degree a large

ADC value is predictive for a malignancy, i.e. the history, demography and clinical picture of the individual patient. Even ADC values of lesions of the same kind show overlap and there is no cut-off value for ADC values in normal parenchyma, benign and malignant lesions. In the literature, ADC values vary between $0.94-2.85 \times 10^{-3} \text{ mm}^2/\text{s}$ for metastases and $0.69-2.28 \times 10^{-3} \text{ mm}^2/\text{s}$ for normal liver parenchyma. This is mainly because every study group uses their own scanning parameters. Differences in b-values are the main cause of non-equivocal results. Breath-hold, respiratory triggered and navigator echo techniques can also give different ADC values. There is need for a uniformly applicable scanning protocol to eliminate discrepancies in ADC values caused by different scanning parameters^[13].

DWI alone is not suitable for the characterization of liver lesions, because solid benign lesions also can show restricted diffusion, and cystic or necrotic malignant lesions have unimpeded diffusion. DWI can help direct the attention of the radiologist to findings that may otherwise be overlooked. Unenhanced and dynamic MRI contrast series alone are very capable in the discrimination of different types of liver lesions, but a combination of DWI and MRI increases the accuracy of the characterization of benign and malignant lesions^[15-17].

Detection of hepatocellular carcinoma

Multiphase multidetector contrast enhanced computed tomography (CT) has reached a high standard for the

Table 1 Reported ADC values in different types of lesions in the liver

Study	Type of lesion	n	ADC value mm ² /s, BH (SD)	ADC value mm ² /s, RT (SD)
Taouli <i>et al</i> ^[10] b-values 0, 50, 500 s/mm ²	Benign	18	2.21 (0.60)	2.39 (0.44)
	Malignant	11	1.04 (0.27)	1.16 (0.33)
Goshima <i>et al</i> ^[13] b-values 100, 200, 400, 800 s/mm ²	Hemangioma	12	1.23-2.23 (0.2-1.2) ²	
	Cyst	15	3.70-4.72 (0.9-1.2) ²	
	Metastases	7	0.99-1.70 (0.5-1.1) ²	
	HCC	21	1.08-1.79 (0.3-10.9) ³	
Kandpal <i>et al</i> ^[14] b-value 0, 500 s/mm ²	Hemangioma	11	2.22 (0.45)	2.36 (0.48)
	Cyst	11	2.66 (0.44)	2.90 (0.51)
	FNH	3	2.03 (0.24)	2.15 (0.18)
	Abscess	6	1.21 (0.36)	1.13 (0.43)
	Metastases	38	1.06 (0.36)	1.13 (0.41)
	HCC	12	1.22 (0.34)	1.27 (0.42)
Gourtsoyianni <i>et al</i> ^[18] b-values 0, 50, 500, 1000 s/mm ²	Hemangioma	7		1.90
	Cyst	15		2.55
	Metastases	13		0.99 (0.22)
	HCC	2		1.38
Oner <i>et al</i> ^[19] b-values 0, 500 s/mm ²	Hemangioma	5	1.72 (0.30)	
	Cyst	3	2.34 (0.36)	
	Metastases	6	1.03 (0.24)	
Demir <i>et al</i> ^[23] 0, 1000 s/mm ²	Benign	24	1.09-3.36 (0.32/0.28) ³	
	Malignant	17	0.54-1.24 (0.07/0.14) ³	
Bruegel <i>et al</i> ^[24] b-values 50, 300, 600 s/mm ²	Hemangioma	56		1.92 (0.34)
	Cyst	51		3.02 (0.31)
	FNH	4		1.40 (0.15)
	Metastases	82		1.22 (0.31)
	HCC	11		1.05 (0.09)
Holzapfel <i>et al</i> ^[25] b-values 50, 300, 600 s/mm ²	Hemangioma	18		1.69 (0.34)
	Cyst	71		2.61 (0.57)
	FNH/adenoma	6/9		1.43 (0.22)
	Metastases	76		1.08 (0.32)
	HCC	17		1.12 (0.28)

¹These studies found significantly higher ADC values in benign liver lesions than in malignant liver lesions; ²This study evaluated the ADC values at different b-values. The lowest and highest ADC values are reported here. The lowest ADC value corresponds with the highest b-value, the highest ADC value with the lowest b-value; ³This study evaluated the ADC values of different types of benign and malignant lesions. The lowest and highest ADC values are reported here. ADC: Apparent diffusion coefficient; BH: Breath-hold; RT: Respiratory triggered; SD: Standard deviation; FNH: Focal nodular hyperplasia; HCC: Hepatocellular carcinoma.

evaluation of the cirrhotic liver and for the detection of hepatocellular carcinoma (HCC). On CT images, diagnosis of HCC is made based on neovascularization with increased arterial enhancement and rapid portal venous wash-out. In the last few years, (liver-specific) contrast enhanced multiphase dynamic MRI has increasingly been used for the detection of HCC. MRI proved to be superior to CT in the detection of HCC and for the characterization of nodules in patients with liver cirrhosis because of the high tissue contrast provided by MRI and the available liver-specific contrast agents. Contrast enhanced MRI is now regarded as the best non-invasive imaging modality. However, even with liver-specific contrast enhanced MRI, there is a diagnostic problem for small HCC lesions (< 10 mm) as well as in

the differentiation from other non-malignant nodules. Large HCC lesions are well-recognized on conventional MRI by their rapid enhancement in the arterial phase and their contrast agent wash-out in the portal-venous phase. Small HCC is less typical on conventional MRI, and differentiation of atypical nodules in the cirrhotic liver is challenging^[27-31].

Xu *et al*^[27,28] found that ADC values were not useful in cirrhotic livers, because cirrhotic parenchyma and solid benign lesions have low ADC values. They cannot be differentiated from lesions with malignant diffusion restriction because of the considerable overlap among their ADC values. Necrosis and vascularization within HCC also alter diffusion, often seen as a false increase in the ADC values.

Zech *et al*^[29] reported a higher sensitivity for DWI compared to conventional MRI in the detection of HCC in the cirrhotic liver (98% for DWI *vs* 83%-85% for MRI). Vandecaveye *et al*^[30] concluded that DWI provided higher sensitivity and positive predictive value for the detection of HCC < 20 mm compared to conventional contrast enhanced MRI (sensitivity and specificity 91.2% and 82.9% *vs* 67.6% and 61.6%, positive predictive value 81.6% and 59.0%, respectively). DWI did not show significantly better results than conventional MRI in detecting HCC > 20 mm. These findings can be explained by the better contrast-to-noise ratio and background suppression of normal liver parenchyma and vascular or bile structures in DWI, which make small lesions more visible, especially when they are in close vicinity to vessels or bile ducts. DWI provides a high negative predictive value on the presence or absence of HCC and reduces the rate of unnecessary invasive diagnostic procedures and follow-up.

Detection of liver metastases

Several studies have demonstrated the usefulness of DWI in the detection of liver metastases. They compared DWI to unenhanced and dynamic liver specific contrast enhanced MRI (Table 2).

Coenegrachts *et al*^[20] showed that lesion conspicuity of hemangiomas and metastases is significantly higher with respiratory triggered DWI at low b-values compared to conventional unenhanced MRI imaging. This is due to an excellent lesion to liver contrast and suppression of background signals from vessels.

Koh *et al*^[32] compared the diagnostic accuracy of DWI and mangafodipir trisodium (MnDPDP)-enhanced MRI alone and in combination in the detection of colorectal liver metastases. They found that a combination of MnDPDP MRI and DWI resulted in the highest diagnostic accuracy (0.94-0.96 *vs* 0.88-0.92 for MnDPDP alone and 0.83-0.90 for DWI alone) with an increased sensitivity, but no loss of specificity. DWI alone is not useful because the sequence is very susceptible to motion artifacts, which obscure lesions and make images difficult to interpret. This is especially the case in the left lobe of the liver. They also stated that experience is needed to interpret DWI correctly, mainly because of the large numbers of artifacts on the images^[33].

Parikh *et al*^[34] reported a significantly higher overall lesion detection rate for breath-hold or respiratory triggered DWI than for conventional T2-weighted MRI (88% *vs* 70%). Bruegel *et al*^[35] compared respiratory DWI-EPI with T2-TSE. They found a sensitivity and specificity for T2-TSE MRI of 45%-62% for unenhanced MRI and 88%-91% for DWI-EPI for lesions > 10 mm. When considering only small metastases < 10 mm, the differences between DWI and conventional MRI with and without contrast are even more pronounced: a sensitivity of 85% for DWI-EPI and 26%-44% for T2-TSE. Lesion detection on T2-TSE is hindered by low lesion to liver contrast and by the interfering bright signal from intrahepatic vessels. Lesion conspicuity with DWI is excellent and limitation

Table 2 Performance of DWI and conventional MRI in the detection of liver metastases *n* (%)

Study	Sensitivity	Specificity	Accuracy	PPV	NPV
Vandecaveye <i>et al</i> ^[30]					
> 20 mm					
B600 SI ratio	100	81.8	94.9	93.3	100
T2-CE MRI	96.4	81.8	92.3	93.1	90.0
< 20 mm					
B600SI ratio	91.2	82.9	86.7	81.6	91.9
T2-CE MRI	67.6	61.0	64.0	59.0	69.4
Koh <i>et al</i> ^[32]					
MnDPDP MRI	81.3	93.0	88-92		
DWI 0, 150, 500 BH	78.3	95.0	83-90		
MnDPDP MRI and DWI	92.2	97.0	94-96		
DWI RT	88-91				
T2 MRI	45-62				
Nasu <i>et al</i> ^[36]					
DWI RT (0, 500)	82	94			
SPIO MRI	66	90			

¹In this study, 2 observers reviewed the images. The given values in sensitivity, specificity and diagnostic accuracy refer to the separate results of both observers. PPV: Positive predictive value; NPV: Negative predictive value.

of the DWI sequence is predominantly referred to lesion characterization rather than to lesion detectability.

Nasu *et al*^[36] assessed the diagnostic accuracy of respiratory triggered DWI in combination with unenhanced MRI *vs* superparamagnetic iron oxide (SPIO)-enhanced imaging. On the basis of a receiver operator characteristic analysis (ROC), averaged over 3 observers, they found a sensitivity and specificity for SPIO-enhanced images of 66% and 90% and for DWI 82% and 94%, respectively.

Predicting response to therapy of primary and secondary liver malignancies by DWI

Tumor responses to chemotherapy and radiation therapy are conventionally assessed by measurement of percentage reduction in tumor size after chemotherapy. However, tumor size measurement on CT or MRI is insensitive to early treatment changes. Theoretically, DWI is sensitive to microenvironmental changes in tumors that occur after treatment. Studies on the predictive value of DWI in primary cancer demonstrated a strong negative correlation between mean pre-treatment ADC values and percentage size reduction of tumors after chemotherapy and chemoradiation. High pretreatment ADC values in tumors were associated with a poor response to chemotherapy^[37,38].

Koh *et al*^[37] showed that high pre-treatment ADC values in colorectal liver metastases were predictive of a poor response to oxaliplatin and 5-fluorouracil-based chemotherapy. They determined with ROC that a mean pretreatment ADC150-500 (ADC map with b-values 150 s/mm² and 500 s/mm²) of 1.69×10^{-3} mm²/s had 60% sensitivity and 100% specificity for identification of non-responding metastatic lesions. They found also a significant linear regression relation between mean ADC150-500 and percentage in tumor size reduction

after treatment. Responding tumors showed a significant increase in ADC values at the end of the treatment. Non-responding tumors and liver parenchyma did not show significant changes in ADC values. Cui *et al.*^[38] analyzed 87 liver metastases of colorectal and gastric origin in 23 patients. They also found significant lower ADC values in responding tumors than in non-responding ones. ADC increased in responding metastases, but not in non-responding ones. They found a weak correlation between tumor size reduction and pretreatment ADC values. The theoretical background for these findings is that higher ADC values are observed in necrotic tissue, and in tissue with loss of cell membrane integrity. When these changes are present before chemotherapy, it may indicate a more aggressive phenotype. Necrotic regions within a tumor are usually poorly perfused, resulting in less delivery of chemotherapeutic agents to these areas. Necrotic regions are also exposed to a more hypoxic and acidic environment, which diminishes the effect of chemotherapy. Necrosis in hepatic metastases is present in almost half of the cases. A possible explanation for non-responding tumors with lower ADC values may be the fact that necrosis is not always associated with high ADC values, especially in the case of coagulation necrosis without cell lysis or liquefaction. The increase in ADC values at the end of the treatment suggests a change from a more cellular pretreatment to a less cellular or necrotic phenotype.

Only one study assessed DWI in HCC treatment with sorafenib. Schraml *et al.*^[39] showed that ADC values with sorafenib, an angiogenesis inhibitor for treatment of HCC, actually showed a decrease instead of an increase. This may be a result of ischemia, induced by inhibition of angiogenesis. The extracellular volume is decreasing, leading to lower ADC values during treatment. They also often observed hemorrhage within the tumors (55%), which may contribute to a decrease in ADC. However, progression of HCC more than 3 mo after therapy was related to a decrease in ADC values. Only conventional MRI could differentiate between hemorrhage and tumor progression. Pre-treatment HCC had high ADC values, because of rich vascularization of the tumors. ADC changes early after chemotherapy seem to reflect the underlying mechanisms in tumor necrosis, most probably hemorrhagic, induced by the novel targeted agent sorafenib early after therapy and may indicate tumor reactivation in the later follow-up period.

DWI after locoregional treatment for liver tumors

Locoregional therapy for liver tumors is used in patients who are not eligible for surgery. The most commonly used local ablative therapies are radiofrequency ablation (RFA) and transcatheter arterial chemoembolization (TACE). The success of these procedures is determined by the rate of ablation site recurrences (ASR), i.e. tumor recurrence as result of incomplete ablation. Close and careful follow-up is needed in patients who underwent treatment by RFA and TACE to detect ASR at an early stage. Unfortunately, diagnostic management remains an issue in these patients,

because of difficulties in differentiating ASR from non-tumoral tissue changes after thermal therapy. Since DWI can provide information about molecular tissue characteristics, it may have an additional value in the evaluation and follow-up of local ablative therapies in patients with liver tumors.

There is one study which evaluated the time-related diffusion alterations after hepatic RFA with regard to potential diagnostic information for the detection of ASR. Schraml *et al.*^[40] reviewed 54 oncological patients treated by RFA for liver metastases from different origins. The ablation zone did not show significant alterations at different time points. Measurement of the ADC value of the entire ablation zone was not suitable for the detection of ASR, because locally changing ADC values were masked by the heterogeneous appearance of the entire ablation zone. Peripheral zones should be analyzed separately. An important technical limitation of ADC measurements after RFA is that the limited spatial resolution does not allow exact ROI positioning in the narrow peripheral rim. Viable tumors after RFA appeared as hyper-intense, and necrotic regions were recognized as hypointense areas on DWI. ASR showed significantly lower ADC values than the ablation zone and normal liver parenchyma ($1.02 \times 10^{-3} \text{ mm}^2/\text{s}$ vs $1.31 \times 10^{-3} \text{ mm}^2/\text{s}$). Suspected areas on DWI were more easily identified and analyzed in conjunction to conventional MR. Signal alterations in the periphery, especially ones with lower ADC values should raise suspicion on ASR. Edema, inflammation, fibrosis and necrosis are associated with higher ADC values. DWI together with conventional imaging is a promising tool in the evaluation of the post-RFA liver and may contribute to the detection of ASR.

The use of DWI after TACE in HCC has recently been investigated. Goshima *et al.*^[41] reported significant increases in ADC values after TACE, but they varied widely and did not contribute to the accurate diagnosis of tumor necrosis by any cut-off points. Yu *et al.*^[42] found that DWI added to conventional MRI could increase the sensitivity for determining ASR especially in the case of atypical lesions. However, they also noticed an increase in the number of false positive findings by adding DWI which affected the overall accuracy of MRI. This was caused by perilesional inflammation and arterial reperfusion of the perilesional atrophic area after TACE. ADC measurement was not helpful for distinguishing viable tumors from perilesional nontumorous changes, since there was great overlap between the ADC values of both entities.

CONCLUSION

DWI in the liver is a relative new and increasingly used imaging technique in addition to conventional unenhanced and contrast enhanced MRI. DWI proved to be helpful in the characterization of focal liver lesions, but should always be used in conjunction with traditional MRI since there is great overlap between ADC values of benign and malignant lesions. DWI is useful in the detection of

small HCC in the cirrhotic liver, with higher sensitivity, specificity and positive predictive value compared to conventional contrast enhanced imaging due to better lesion to liver contrast and background suppression of signals arising from vessels and bile ducts. This is also the case for the detection of metastases in the liver. However, it should be noted that DWI images are difficult to interpret since DWI is very sensitive to artifacts. It seems reasonable to use DWI in conjunction to conventional imaging. DWI is not yet commonly used in the follow-up after treatment of liver malignancies. Pre-treatment ADC values in tumors treated with chemotherapy seem to be useful in the prediction and evaluation of the treatment response of primary and secondary liver malignancies. DWI in the follow-up after RFA and TACE shows promising results in the detection of ablation site recurrences, especially in combination with conventional contrast enhanced imaging.

REFERENCES

- Bammer R.** Basic principles of diffusion-weighted imaging. *Eur J Radiol* 2003; **45**: 169-184
- Naganawa S,** Kawai H, Fukatsu H, Sakurai Y, Aoki I, Miura S, Mimura T, Kanazawa H, Ishigaki T. Diffusion-weighted imaging of the liver: technical challenges and prospects for the future. *Magn Reson Med Sci* 2005; **4**: 175-186
- Charles-Edwards EM,** deSouza NM. Diffusion-weighted magnetic resonance imaging and its application to cancer. *Cancer Imaging* 2006; **6**: 135-143
- Thoeny HC,** De Keyzer F. Extracranial applications of diffusion-weighted magnetic resonance imaging. *Eur Radiol* 2007; **17**: 1385-1393
- Kwee TC,** Takahara T, Ochiai R, Nievelstein RA, Luijten PR. Diffusion-weighted whole-body imaging with background body signal suppression (DWIBS): features and potential applications in oncology. *Eur Radiol* 2008; **18**: 1937-1952
- Koh DM,** Takahara T, Imai Y, Collins DJ. Practical aspects of assessing tumors using clinical diffusion-weighted imaging in the body. *Magn Reson Med Sci* 2007; **6**: 211-224
- Le Bihan D,** Poupon C, Amadon A, Lethimonnier F. Artifacts and pitfalls in diffusion MRI. *J Magn Reson Imaging* 2006; **24**: 478-488
- Kwee TC,** Takahara T, Ochiai R, Katahira K, Van Cauteren M, Imai Y, Nievelstein RA, Luijten PR. Whole-body diffusion-weighted magnetic resonance imaging. *Eur J Radiol* 2009; **70**: 409-417
- Ivancevic MK,** Kwee TC, Takahara T, Ogino T, Hussain HK, Liu PS, Chenevert TL. Diffusion-weighted MR imaging of the liver at 3.0 Tesla using TRacking Only Navigator echo (TRON): a feasibility study. *J Magn Reson Imaging* 2009; **30**: 1027-1033
- Taouli B,** Sandberg A, Stemmer A, Parikh T, Wong S, Xu J, Lee VS. Diffusion-weighted imaging of the liver: comparison of navigator triggered and breathhold acquisitions. *J Magn Reson Imaging* 2009; **30**: 561-568
- Yoshikawa T,** Ohno Y, Kawamitsu H, Ku Y, Seo Y, Zamora CA, Aoyama N, Sugimura K. Abdominal apparent diffusion coefficient measurements: effect of diffusion-weighted image quality and usefulness of anisotropic images. *Magn Reson Imaging* 2008; **26**: 1415-1420
- Kwee TC,** Takahara T, Niwa T, Ivancevic MK, Herigault G, Van Cauteren M, Luijten PR. Influence of cardiac motion on diffusion-weighted magnetic resonance imaging of the liver. *MAGMA* 2009; **22**: 319-325
- Goshima S,** Kanematsu M, Kondo H, Yokoyama R, Kajita K, Tsuge Y, Watanabe H, Shiratori Y, Onozuka M, Moriyama N. Diffusion-weighted imaging of the liver: optimizing b value for the detection and characterization of benign and malignant hepatic lesions. *J Magn Reson Imaging* 2008; **28**: 691-697
- Kandpal H,** Sharma R, Madhusudhan KS, Kapoor KS. Respiratory-triggered versus breath-hold diffusion-weighted MRI of liver lesions: comparison of image quality and apparent diffusion coefficient values. *AJR Am J Roentgenol* 2009; **192**: 915-922
- Feuerlein S,** Pauls S, Juchems MS, Stuber T, Hoffmann MH, Brambs HJ, Ernst AS. Pitfalls in abdominal diffusion-weighted imaging: how predictive is restricted water diffusion for malignancy. *AJR Am J Roentgenol* 2009; **193**: 1070-1076
- Sandrasegaran K,** Akisik FM, Lin C, Tahir B, Rajan J, Aisen AM. The value of diffusion-weighted imaging in characterizing focal liver masses. *Acad Radiol* 2009; **16**: 1208-1214
- Lichy MP,** Aschoff P, Plathow C, Stemmer A, Horger W, Mueller-Horvat C, Steidle G, Horger M, Schafer J, Eschmann SM, Kiefer B, Claussen CD, Pfannenbergl C, Schlemmer HP. Tumor detection by diffusion-weighted MRI and ADC-mapping--initial clinical experiences in comparison to PET-CT. *Invest Radiol* 2007; **42**: 605-613
- Gourtsoyianni S,** Papanikolaou N, Yarmenitis S, Maris T, Karantanis A, Gourtsoyiannis N. Respiratory gated diffusion-weighted imaging of the liver: value of apparent diffusion coefficient measurements in the differentiation between most commonly encountered benign and malignant focal liver lesions. *Eur Radiol* 2008; **18**: 486-492
- Oner AY,** Celik H, Oktar SO, Tali T. Single breath-hold diffusion-weighted MRI of the liver with parallel imaging: initial experience. *Clin Radiol* 2006; **61**: 959-965
- Coenegrachts K,** Delanote J, Ter Beek L, Haspelslagh M, Bipat S, Stoker J, Van Kerkhove F, Steyaert L, Rigauts H, Casselman JW. Improved focal liver lesion detection: comparison of single-shot diffusion-weighted echoplanar and single-shot T2 weighted turbo spin echo techniques. *Br J Radiol* 2007; **80**: 524-531
- Low RN,** Gurney J. Diffusion-weighted MRI (DWI) in the oncology patient: value of breathhold DWI compared to unenhanced and gadolinium-enhanced MRI. *J Magn Reson Imaging* 2007; **25**: 848-858
- Asbach P,** Hein PA, Stemmer A, Wagner M, Huppertz A, Hamm B, Taupitz M, Klessen C. Free-breathing echo-planar imaging based diffusion-weighted magnetic resonance imaging of the liver with prospective acquisition correction. *J Comput Assist Tomogr* 2008; **32**: 372-378
- Demir OI,** Obuz F, Sağol O, Dicle O. Contribution of diffusion-weighted MRI to the differential diagnosis of hepatic masses. *Diagn Interv Radiol* 2007; **13**: 81-86
- Bruegel M,** Holzapfel K, Gaa J, Woertler K, Waldt S, Kiefer B, Stemmer A, Ganter C, Rummeny EJ. Characterization of focal liver lesions by ADC measurements using a respiratory triggered diffusion-weighted single-shot echoplanar MR imaging technique. *Eur Radiol* 2008; **18**: 477-485
- Holzapfel K,** Bruegel M, Eiber M, Ganter C, Schuster T, Heinrich P, Rummeny EJ, Gaa J. Characterization of small (≤ 10 mm) focal liver lesions: Value of respiratory-triggered echo-planar diffusion-weighted MR imaging. *Eur J Radiol* 2009; Epub ahead of print
- Coenegrachts K,** Matos C, ter Beek L, Metens T, Haspelslagh M, Bipat S, Stoker J, Rigauts H. Focal liver lesion detection and characterization: comparison of non-contrast enhanced and SPIO-enhanced diffusion-weighted single-shot spin echo echo planar and turbo spin echo T2-weighted imaging. *Eur J Radiol* 2009; **72**: 432-439
- Xu H,** Li X, Xie JX, Yang ZH, Wang B. Diffusion-weighted magnetic resonance imaging of focal hepatic nodules in an experimental hepatocellular carcinoma rat model. *Acad Radiol* 2007; **14**: 279-286

- 28 **Xu PJ**, Yan FH, Wang JH, Lin J, Ji Y. Added value of breathhold diffusion-weighted MRI in detection of small hepatocellular carcinoma lesions compared with dynamic contrast-enhanced MRI alone using receiver operating characteristic curve analysis. *J Magn Reson Imaging* 2009; **29**: 341-349
- 29 **Zech CJ**, Reiser MF, Herrmann KA. Imaging of hepatocellular carcinoma by computed tomography and magnetic resonance imaging: state of the art. *Dig Dis* 2009; **27**: 114-124
- 30 **Vandecaveye V**, De Keyzer F, Verslype C, Op de Beeck K, Komuta M, Topal B, Roebben I, Bielen D, Roskams T, Nevens F, Dymarkowski S. Diffusion-weighted MRI provides additional value to conventional dynamic contrast-enhanced MRI for detection of hepatocellular carcinoma. *Eur Radiol* 2009; **19**: 2456-2466
- 31 **Willatt JM**, Hussain HK, Adusumilli S, Marrero JA. MR Imaging of hepatocellular carcinoma in the cirrhotic liver: challenges and controversies. *Radiology* 2008; **247**: 311-330
- 32 **Koh DM**, Brown G, Riddell AM, Scurr E, Collins DJ, Allen SD, Chau I, Cunningham D, deSouza NM, Leach MO, Husband JE. Detection of colorectal hepatic metastases using MnDPDP MR imaging and diffusion-weighted imaging (DWI) alone and in combination. *Eur Radiol* 2008; **18**: 903-910
- 33 **Koh DM**, Scurr E, Collins DJ, Pirgon A, Kanber B, Karanjia N, Brown G, Leach MO, Husband JE. Colorectal hepatic metastases: quantitative measurements using single-shot echo-planar diffusion-weighted MR imaging. *Eur Radiol* 2006; **16**: 1898-1905
- 34 **Parikh T**, Drew SJ, Lee VS, Wong S, Hecht EM, Babb JS, Taouli B. Focal liver lesion detection and characterization with diffusion-weighted MR imaging: comparison with standard breath-hold T2-weighted imaging. *Radiology* 2008; **246**: 812-822
- 35 **Bruegel M**, Rummeny EJ. Hepatic metastases: use of diffusion-weighted echo-planar imaging. *Abdom Imaging* 2009; Epub ahead of print
- 36 **Nasu K**, Kuroki Y, Nawano S, Kuroki S, Tsukamoto T, Yamamoto S, Motoori K, Ueda T. Hepatic metastases: diffusion-weighted sensitivity-encoding versus SPIO-enhanced MR imaging. *Radiology* 2006; **239**: 122-130
- 37 **Koh DM**, Scurr E, Collins D, Kanber B, Norman A, Leach MO, Husband JE. Predicting response of colorectal hepatic metastasis: value of pretreatment apparent diffusion coefficients. *AJR Am J Roentgenol* 2007; **188**: 1001-1008
- 38 **Cui Y**, Zhang XP, Sun YS, Tang L, Shen L. Apparent diffusion coefficient: potential imaging biomarker for prediction and early detection of response to chemotherapy in hepatic metastases. *Radiology* 2008; **248**: 894-900
- 39 **Schraml C**, Schwenzer NF, Martirosian P, Bitzer M, Lauer U, Claussen CD, Horger M. Diffusion-weighted MRI of advanced hepatocellular carcinoma during sorafenib treatment: initial results. *AJR Am J Roentgenol* 2009; **193**: W301-W307
- 40 **Schraml C**, Schwenzer NF, Clasen S, Rempp HJ, Martirosian P, Claussen CD, Pereira PL. Navigator respiratory-triggered diffusion-weighted imaging in the follow-up after hepatic radiofrequency ablation-initial results. *J Magn Reson Imaging* 2009; **29**: 1308-1316
- 41 **Goshima S**, Kanematsu M, Kondo H, Yokoyama R, Tsuge Y, Shiratori Y, Onozuka M, Moriyama N. Evaluating local hepatocellular carcinoma recurrence post-transcatheter arterial chemoembolization: is diffusion-weighted MRI reliable as an indicator? *J Magn Reson Imaging* 2008; **27**: 834-839
- 42 **Yu JS**, Kim JH, Chung JJ, Kim KW. Added value of diffusion-weighted imaging in the MRI assessment of perilesional tumor recurrence after chemoembolization of hepatocellular carcinomas. *J Magn Reson Imaging* 2009; **30**: 153-160

S- Editor Tian L L- Editor Cant MR E- Editor Ma WH